ese studies have concentrated on the
ll or zero. The curve $F_0 = 0$ of Figure
ced by the ship are confined within a
sin (1/3) = 19.5°, spanning the ship's
in ship-wake wedge angle, and is also
s by the group velocity vector at the
mber curve; all other group velocity
, so that the corresponding waves lie
to the boundary of the wedge have a
d the region is an example of a *caustic*
with no waves and a region where two
. The wave field is evanescent outside
structure at the caustic, which implies
eyond the Kelvin wedge angle (Light-

produced by boats and ships show
t generate waves with a spectrum of
minant wavenumber $k \sim 2\pi/L$, where
r these waves, (2.2.32) gives

$$\left(\frac{2\pi U^2}{gL}\right)^2 - 1\Bigg]^{1/2}. \qquad (2.2.33)$$

an liner or large container vessel, the
small m and are transverse, behind the
$^2/gL \gg 1$, as for a speedboat, (2.2.33)
en concentrated in a wedge of angular
s much less than the Kelvin angle α_K,
t a similarly small angle to the boat's

angle increases and the (theoretically
that wakes noticeably wider than the
ed for $F_0 \gtrsim 0.7$. For $F_0 \gtrsim 1$, the caustic
mbles the hydrostatic wake described
w close to 90°, but it decreases as F_0
to the Kelvin wake angle as $F_0 \to 3$.
en $F_0 > 3$, where the wake is confined
h narrows to zero as F_0 increases to
f small craft at high speed with $F_0 \ll 1$,
nes been incorrectly attributed to shal-
in the past. Ship wake situations where
ther than the rule, but *are* possible in

shallow water (for example, $F_0 = 1$ for ship (or boat) speed $U =$ 28 knots in water of 20 m depth). For the case of forcing by topography, where U is the current speed, Froude numbers of order unity are common in shallow, fast-moving streams, and the resulting non-linear effects are discussed in the following sections. But for most of the time, for most rivers, the Froude numbers are small. In the stratified analogues to be discussed in subsequent chapters, and which are our primary concern, Froude numbers of all values are possible.

I am not aware of any detailed observational tests of the linear theory for two-dimensional ship wakes, but the latter gives a good qualitative description of the disturbances produced by ducks, boats etc. (Examples are shown in Stoker 1957 and Lighthill 1978.) For flow over topography, there is no reason to question the validity of linear theory for sufficiently small h, but this range of validity is dependent on F_0.

2.3 One-dimensional non-linear hydrostatic flow

We now return to one-dimensional flow and investigate non-linear effects. These phenomena are most readily appreciated in the hydrostatic system with its long horizontal length-scales, where dispersive effects are not present. From (2.1.6, 2.1.8) we obtain for this system, with $d = d_0 + \eta - h$,

$$u_t + uu_x = -g\eta_x, \qquad (2.3.1)$$

$$d_t + (du)_x = 0, \qquad (2.3.2)$$

or alternatively

$$\eta_t + [(d_0 + \eta)u]_x = (uh)_{x'} \qquad (2.3.3)$$

and we again take the initial conditions (2.2.3), namely $u = U$, $\eta = h$, $\eta_t = 0$, at $t = 0$. This is a classic system of hyperbolic diffential equations with a forcing term, which may be expressed in the characteristic form

$$\frac{\mathrm{d}}{\mathrm{d}t}(u \pm 2\sqrt{gd}) = -g\frac{\mathrm{d}h}{\mathrm{d}x}, \qquad (2.3.4)$$

on the respective characteristic curves, which are given by

$$\frac{\mathrm{d}x}{\mathrm{d}t} = u \pm \sqrt{gd}. \qquad (2.3.5)$$

(For a discussion of this type of mathematical system, see Whitham 1974; an interesting geometrical approach has been described by Broad *et al*. 1993). For small times, the solution of this initial-value problem is essentially the same as for the linear system, and it is given by (2.2.5) and displayed in Figure 2.1. The flow is still governed by the value of the Froude number for the undisturbed flow $F_0 = U/\sqrt{gd_0}$, but as time increases the characteristics over the obstacle do not remain straight but become curved, depending on the values of the flow variables u and d. Representative examples for $F_0 < 1$ and $F_0 > 1$, showing the characteristics of the upstream-propagating waves only, are presented in Figure 2.6. In most situations of interest, the downstream-propagating wave (on the characteristics $\mathrm{d}x/\mathrm{d}t = u + \sqrt{gd}$) is little affected by non-linearities, and travels quickly downstream away from the vicinity of the obstacle. Whilst necessary to satisfy the initial conditions, these waves are unimportant otherwise and are not relevant to the following discussion. However, on the upstream side of the obstacle, the equations for the variables on this same family of characteristics ((2.3.4, 2.3.5) with the plus sign) may be integrated to yield

$$u + 2\sqrt{gd} = U + 2\sqrt{gd_0}, \tag{2.3.6}$$

since the initial conditions are the same for each member of this family of characteristics on the upstream side. Substituting (2.3.6) into (2.3.4, 2.3.5) then yields, for the other set of characteristics (for waves propagating against the flow),

$$\frac{\mathrm{d}u}{\mathrm{d}t} = \frac{\mathrm{d}d}{\mathrm{d}t} = 0, \quad \text{on } \frac{\mathrm{d}x}{\mathrm{d}t} = U + 2\sqrt{gd_0} - 3\sqrt{gd}, \tag{2.3.7}$$

on the upstream side of the obstacle. In this region, d is constant on each characteristic which is therefore straight, but the slopes are different for different characteristics. The result is that, for $F_0 > 1$, the characteristics converge and intersect, as shown in Figure 2.6a, because a disturbance of larger elevation travels faster. For $F_0 > 1$ the effect may be large enough to cause the upstream waves over the obstacle to change direction, as shown in Figure 2.6b. The same processes occur, *mutatis mutandis*, on the downstream side.

This phenomenon of wave speed being dependent on wave amplitude is termed *amplitude dispersion*, and is illustrated in a simpler form in Figure 2.7. A wave of elevation, here simplified to a monotonic increase in surface level moving to the left into undisturbed fluid, is also governed by (2.3.6) and (2.3.7), which show that the interface steepens with time as shown in Figure 2.7a. On the other hand, a decrease in surface level moving in the same direction and leaving

he solution of this initial-value problem
ɛ linear system, and it is given by (2.2.5)
ıe flow is still governed by the value of
ndisturbed flow $F_0 = U/\sqrt{gd_0}$, but as
tics over the obstacle do not remain
depending on the values of the flow
ative examples for $F_0 < 1$ and $F_0 > 1$,
the upstream-propagating waves only,
ı most situations of interest, the down-
he characteristics $\mathrm{d}x/\mathrm{d}t = u + \sqrt{gd})$ is
;, and travels quickly downstream away
e. Whilst necessary to satisfy the initial
ıimportant otherwise and are not rele-
ı. However, on the upstream side of the
he variables on this same family of
ith the plus sign) may be integrated to

$$\overline{d} = U + 2\sqrt{gd_0}, \qquad (2.3.6)$$

he same for each member of this family
am side. Substituting (2.3.6) into (2.3.4),
ther set of characteristics (for waves

$$\frac{\mathrm{d}x}{\mathrm{d}t} = U + 2\sqrt{gd_0} - 3\sqrt{gd}, \qquad (2.3.7)$$

ɔstacle. In this region, d is constant on
herefore straight, but the slopes are
istics. The result is that, for $F_0 > 1$, the
ersect, as shown in Figure 2.6a, because
on travels faster. For $F_0 > 1$ the effect
he upstream waves over the obstacle to
Figure 2.6b. The same processes occur,
stream side.
speed being dependent on wave am-
spersion, and is illustrated in a simpler
f elevation, here simplified to a mono-
ıoving to the left into undisturbed fluid,
l (2.3.7), which show that the interface
in Figure 2.7a. On the other hand, a
ing in the same direction and leaving

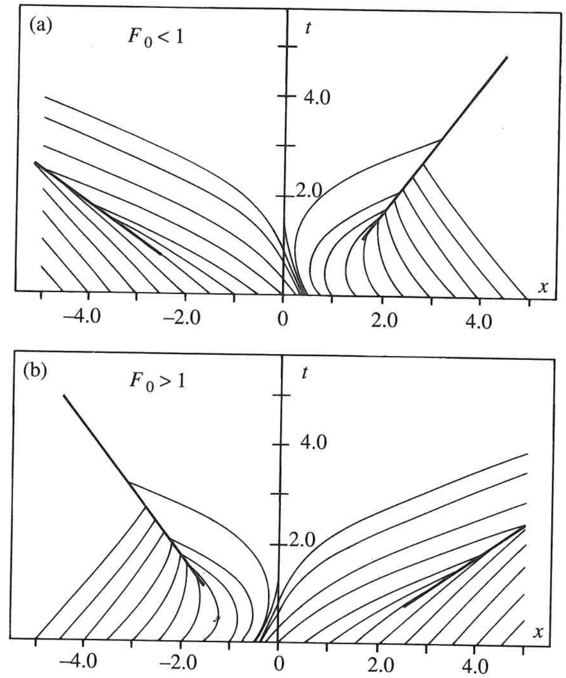

Fig. 2.6. Representative characteristics for the upstream-propagating disturbances for non-linear hydrostatic flow forced by an obstacle impulsively set into motion, when upstream jumps form (cf. Figure 2.1). The obstacle is centred at $x = 0$, and decreases in height to near-zero at $x = \pm 3$. The jumps are denoted by heavy lines. (a) $F_0 < 1$, (b) $F_0 > 1$. (Adapted from Grimshaw & Smyth 1986.)

shallower fluid at rest on the right becomes more spread out, or "rarefied", with time, as shown in Figure 2.7b. The upstream wave of elevation produced by the starting motion of the obstacle therefore steepens, to the point where the interface becomes vertical, and in principle overturns. Within the framework of the present model, this results in a "hydraulic jump" which may be modelled as a discontinuity, and it is not governed by the above equations *per se*. Hence we must consider its behaviour as an independent entity.

2.3.1 Hydraulic jumps

We consider a simple model of hydraulic jumps based on the principles of mass and momentum conservation, which will be adequate for our present purposes. More detailed properties of jumps will be discussed later in this chapter. We assume that a hydraulic jump may be

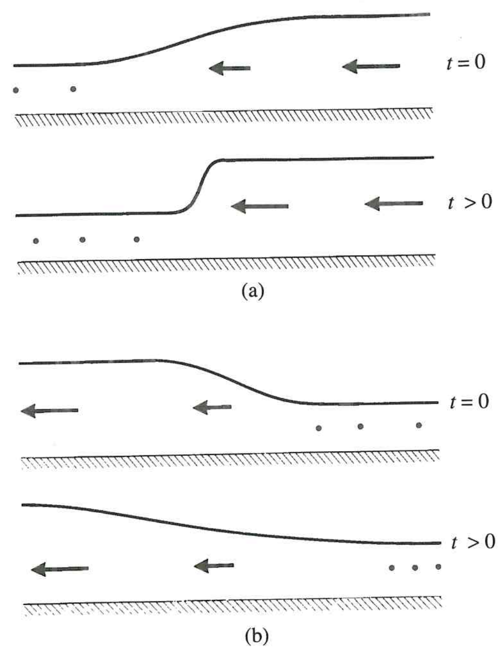

Fig. 2.7. The development of a moving surge according to the hydraulic model. (a) A monotonic increase in depth where the deeper fluid is moving to the left at $t = 0$ into fluid at rest, steepens at subsequent times to form a discontinuity or bore. Arrow length denotes speed of fluid, and dots denote fluid at rest. (b) The reverse situation where the deeper fluid moves away from the depth change, leaving fluid at rest on the right. At later times this disturbance is more spread out, or "rarefied".

regarded as a locally steady and compact region with its own internal dynamics, which may be modelled as a discontinuity between two uniform streams, and that it is produced as a result of wave steepening as just described. We then require equations relating conditions on the upstream and downstream sides of the jump, which must be considered from first principles. At the most fundamental level, we must have conservation of mass and momentum in the region of fluid containing the jump. We take coordinates fixed relative to the jump, and in this frame of reference denote the fluid velocity and depth on the upstream side by u_u and d_u, and on the downstream side by u_d and d_d, as shown in Figure 2.8. Conservation of mass into and out of the jump then gives

$$u_u d_u = u_d d_d = Q, \tag{2.3.8}$$

where Q is the volume flux relative to the jump. Conservation of momentum applied to a vertical column of fluid implies that the

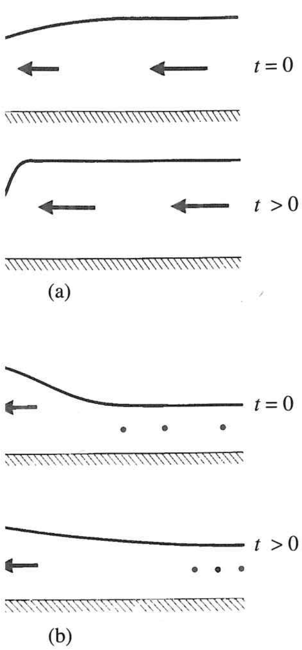

ving surge according to the hydraulic model.
where the deeper fluid is moving to the left
s at subsequent times to form a discontinuity
ed of fluid, and dots denote fluid at rest. (b)
deeper fluid moves away from the depth
right. At later times this disturbance is more

nd compact region with its own internal
delled as a discontinuity between two
produced as a result of wave steepening
uire equations relating conditions on the
s of the jump, which must be considered
most fundamental level, we must have
nentum in the region of fluid containing
s fixed relative to the jump, and in this
fluid velocity and depth on the upstream
downstream side by u_d and d_d, as shown
mass into and out of the jump then gives

$$_{u} = u_d d_d = Q, \qquad (2.3.8)$$

relative to the jump. Conservation of
tical column of fluid implies that the

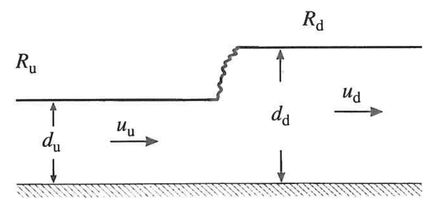

Fig. 2.8. Notation in the frame of a steady hydraulic jump (see text).

vertically integrated form of (2.3.1) applies across the jump, and integrating (2.3.1) vertically and then horizontally gives

$$d_u u_u^2 + \tfrac{1}{2} g d_u^2 = d_d u_d^2 + \tfrac{1}{2} g d_d^2. \qquad (2.3.9)$$

These two equations completely specify the properties of the jump at this level of approximation, and enable relevant properties to be calculated. One of these is the rate of energy dissipation within the jump. The energy density of a column of fluid is given by

$$E = \tfrac{1}{2}\rho_0 d u^2 + \tfrac{1}{2}\rho_0 g d^2, \qquad (2.3.10)$$

and from (2.3.1, 2.3.2), over level ground the rate of change of energy is given by

$$\frac{\partial E}{\partial t} = -\frac{\partial}{\partial x}\rho_0\left(\tfrac{1}{2} d u^3 + g u d^2\right) = -\frac{\partial}{\partial x}\rho_0 Q R, \qquad (2.3.11)$$

where $\rho_0 Q R = \rho_0 d u (u^2/2 + g d)$ may be identified as the *flux* of energy. Note that the flux of energy is not simply given by uE, because each fluid column is not independent of the others, and account must be taken of work done by the pressure force that acts between them (see (1.3.3–6)). The rate of energy dissipation within the jump is then given by the differences between the energy fluxes into and out of the jump, namely

$$\frac{dE_J}{dt} = \rho_0 Q(R_u - R_d) = \frac{\rho_0 g Q}{4}\frac{(d_d - d_u)^3}{d_d d_u}, \qquad (2.3.12)$$

where E_J denotes the energy of the fluid in a region containing the jump and moving with it. The mechanisms for this energy dissipation depend on the detailed internal dynamics of the jump, and (2.3.12) is effectively a requirement imposed by the external conditions. Note that for the energy dissipation to be positive we must have $d_d > d_u$.

For a jump advancing into water that is at rest, the speed of the jump in this frame, c_J, is given by $u_u = c_J$, and eliminating u_d from (2.3.8, 2.3.9) yields

$$c_J^2 = \frac{g d_d}{2}\left(1 + \frac{d_d}{d_u}\right), \qquad (2.3.13)$$

a speed which is faster than that of linear waves on fluid of depth d_d (where wave speed $c = \sqrt{gd_d}$), because the fluid following the jump is moving in the same direction in this reference frame.

2.3.2 Flow solutions with topography

The steady-state flow solutions may be specified by the two dimensionless parameters F_0 and $H_m = h_m/d_0$, where h_m is the maximum height of the topography. If h_m is sufficiently small the solution is approximately linear, as described by (2.2.5). Here, when $F_0 < 1$ the upstream disturbance escapes from the region of the obstacle, and for $F_0 > 1$, the corresponding wave is advected away downstream. In both cases, we are left with a steady disturbance over the obstacle, where the upstream conditions are unchanged from the initial ones of $u = U$, $d = d_0$. The steady-state forms of (2.3.1, 2.3.2) may be expressed as

$$\frac{\mathrm{d}}{\mathrm{d}x}\left(\tfrac{1}{2}u^2 + gd + gh\right) = 0, \quad \frac{\mathrm{d}}{\mathrm{d}x}(ud) = 0, \tag{2.3.14}$$

which give

$$ud = Q = Ud_0, \tag{2.3.15}$$

and

$$\tfrac{1}{2}u^2 + gd + gh = \frac{Q^2}{2d^2} + gd + gh = \tfrac{1}{2}U^2 + gd_0, \tag{2.3.16}$$

which gives $d(x)$ as a function of $h(x)$. This equation may be expressed as

$$\tfrac{1}{2}\left(\frac{F_0 d_0}{d}\right)^2 + \frac{d}{d_0} + \frac{h}{d_0} = \tfrac{1}{2}F_0^2 + 1, \tag{2.3.17}$$

and the solutions are qualitatively similar to those obtained from linear theory (2.2.5) and shown in Figure 2.1. The range of applicability of (2.3.16, 2.3.17) is limited, though, and the limit is seen from (2.3.14) which gives

$$\left(\frac{u^2}{gd} - 1\right)\frac{\mathrm{d}d}{\mathrm{d}x} = \frac{\mathrm{d}h}{\mathrm{d}x}. \tag{2.3.18}$$

This implies that at the crest of a single-humped obstacle where $\mathrm{d}h/\mathrm{d}x$ vanishes, either $\mathrm{d}d/\mathrm{d}x$ also vanishes or the local Froude number F, defined by $F^2 = u^2/gd$, is unity. Also, when $F = 1$ we must have $\mathrm{d}h/\mathrm{d}x = 0$. Now in these steady solutions we have $F = F_0$ upstream, and for $F_0 < 1$, F increases over the obstacle as d decreases and u increases with increasing h. But from (2.3.18), F can only equal unity at the crest of the obstacle where h has its maximum value, h_m. Hence